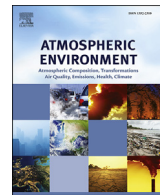




Contents lists available at ScienceDirect

Atmospheric Environment

journal homepage: www.elsevier.com/locate/atmosenv

Correlations between short-term mobile monitoring and long-term passive sampler measurements of traffic-related air pollution



Erin A. Riley ^{a,*}, LaNae Schaal ^b, Miyoko Sasakura ^a, Robert Crampton ^a,
 Timothy R. Gould ^c, Kris Hartin ^a, Lianne Sheppard ^{a,b}, Timothy Larson ^{a,c},
 Christopher D. Simpson ^a, Michael G. Yost ^a

^a University of Washington Department of Environmental and Occupational Health Sciences, Box 357234, Seattle, WA 98198, USA^b University of Washington Department of Biostatistics, Box 357232, Seattle, WA 98198, USA^c University of Washington Department of Civil & Environmental Engineering, Box 352700, Seattle, WA 98198, USA

HIGHLIGHTS

- A city wide mobile monitoring campaign was combined with passive samplers.
- Correlations between mobile and passive measurements were moderate to strong.
- Short term mobile monitoring may be representative of long term spatial patterns.

ARTICLE INFO

Article history:

Received 20 September 2015

Received in revised form

29 February 2016

Accepted 2 March 2016

Available online 2 March 2016

Keywords:

Traffic-related air pollution

Mobile monitoring

Ozone

Ultrafine particles

Black carbon

ABSTRACT

Mobile monitoring has provided a means for broad spatial measurements of air pollutants that are otherwise impractical to measure with multiple fixed site sampling strategies. However, the larger the mobile monitoring route the less temporally dense measurements become, which may limit the usefulness of short-term mobile monitoring for applications that require long-term averages. To investigate the stationarity of short-term mobile monitoring measurements, we calculated long term medians derived from a mobile monitoring campaign that also employed 2-week integrated passive sampler detectors (PSD) for NO_x, Ozone, and nine volatile organic compounds at 43 intersections distributed across the entire city of Baltimore, MD. This is one of the largest mobile monitoring campaigns in terms of spatial extent undertaken at this time. The mobile platform made repeat measurements every third day at each intersection for 6–10 min at a resolution of 10 s. In two-week periods in both summer and winter seasons, each site was visited 3–4 times, and a temporal adjustment was applied to each dataset. We present the correlations between eight species measured using mobile monitoring and the 2-week PSD data and observe correlations between mobile NO_x measurements and PSD NO_x measurements in both summer and winter (Pearson's $r = 0.84$ and 0.48, respectively). The summer season exhibited the strongest correlations between multiple pollutants, whereas the winter had comparatively few statistically significant correlations. In the summer CO was correlated with PSD pentanes ($r = 0.81$), and PSD NO_x was correlated with mobile measurements of black carbon ($r = 0.83$), two ultrafine particle count measures ($r = 0.8$), and intermodal (1–3 μm) particle counts ($r = 0.73$). Principal Component Analysis of the combined PSD and mobile monitoring data revealed multipollutant features consistent with light duty vehicle traffic, diesel exhaust and crankcase blow by. These features were more consistent with published source profiles of traffic-related air pollutants than features based on the PSD data alone. Short-term mobile monitoring shows promise for capturing long-term spatial patterns of traffic-related air pollution, and is complementary to PSD sampling strategies.

© 2016 Elsevier Ltd. All rights reserved.

1. Introduction

* Corresponding author.

E-mail address: eriley1@uw.edu (E.A. Riley).

Mobile monitoring has been commonly used to investigate the

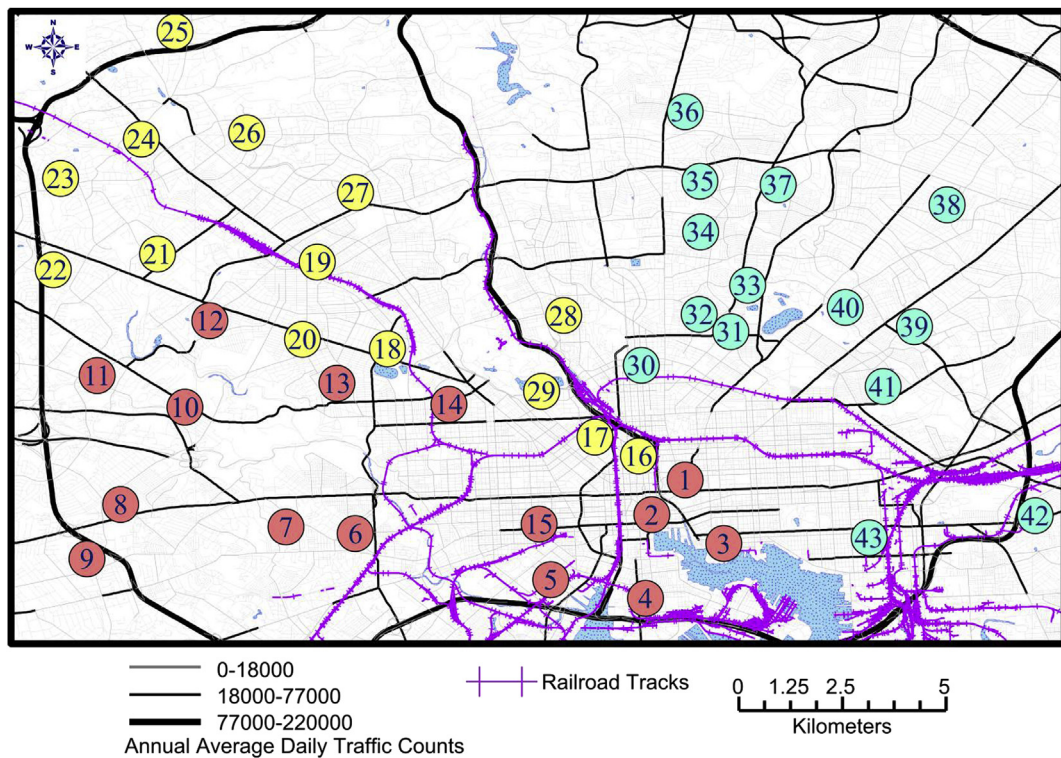


Fig. 1. Map of the study area. Fixed routes were driven for each colored subset of locations, with each route driven every third day. Map produced using ArcMap (ESRI Inc., 2014), railroad data from Open Baltimore, map layers from US census (Geography Division, 2008), and traffic counts from Maryland department of transportation (State Highway Administration, 2012).

spatial distributions of traffic-related air pollutants (TRAP); however, mobile monitoring campaigns are resource intensive and are therefore typically limited in duration or require restricted spatial coverage to allow for both temporal and spatial density of data. A concern for using mobile monitoring data in a regulatory framework is establishing how representative short-term monitoring data are of longer-term spatial averages obtained by conventional methods (Van den Bossche et al., 2015). To address this concern, we present an investigation into the stationarity of mobile monitoring data relative to fixed integrated passive sampler detectors (PSDs), as well as the added benefit of conducting both types of monitoring concurrently.

Both mobile monitoring and fixed sampler detection schemes (passive and continuous) have been used to refine predictive

models for criteria pollutants and, more recently, for pollutants of emerging concern such as black carbon (Dons et al., 2013b) and ultrafine particle counts. Passive sampler detectors (PSD) adsorb air pollutants directly from the environment. PSDs are advantageous for their simplicity of use, and in the case of volatile organic compounds (VOCs), their ability to detect a large number of chemicals with a single sampler. However, the temporal resolution of PSDs is limited by analytical detection limits, and temperature-dependent sampling rates. When used for ambient monitoring PSDs typically require several days to collect a sample, and can be deployed for up to two weeks before saturation (Beckerman et al., 2008; Cohen et al., 2009).

Mobile monitoring platforms have now been developed for pedestrians (Marc et al., 2012; Dons et al., 2013a), bicycles

Table 1

List of species on mobile platform and passive sample detectors (PSD).

Mobile platform		PSD	
Species	Units used	Species	Units used
UFPN (diameter 25–400 nm)	Counts/liter	Pentanes (includes pentanes and hexanes ^b)	µg/m ³ (multiply by 100 to achieve original conc)
PN ₁ (diameter 50–1000 nm)	Counts/liter	Benzene	µg/m ³
PN _{fine} (diameter 0.25–1 µm)	Counts/liter	Toluene	µg/m ³
Intermodal PN (1–3 µm)	Counts/liter	m-Xylene	µg/m ³
Black Carbon (BC)	ng/m ³	o-Xylene	µg/m ³
NO _x	ppb	Nonane	µg/m ³
CO (summer only) ^a	ppm	Decane	µg/m ³
O ₃	mg/m ³	Undecane	µg/m ³
Volatile Organic Compounds (VOCs)	ppm	Dodecane (Winter Only) ^a	µg/m ³
		NO _x	ppb
		NO ₂	ppb
		O ₃	ppb

^a Missing data in the case of winter CO, and laboratory error for summer Dodecane.

^b See section S3.2.3 in the supplemental material for quantification of pentanes.

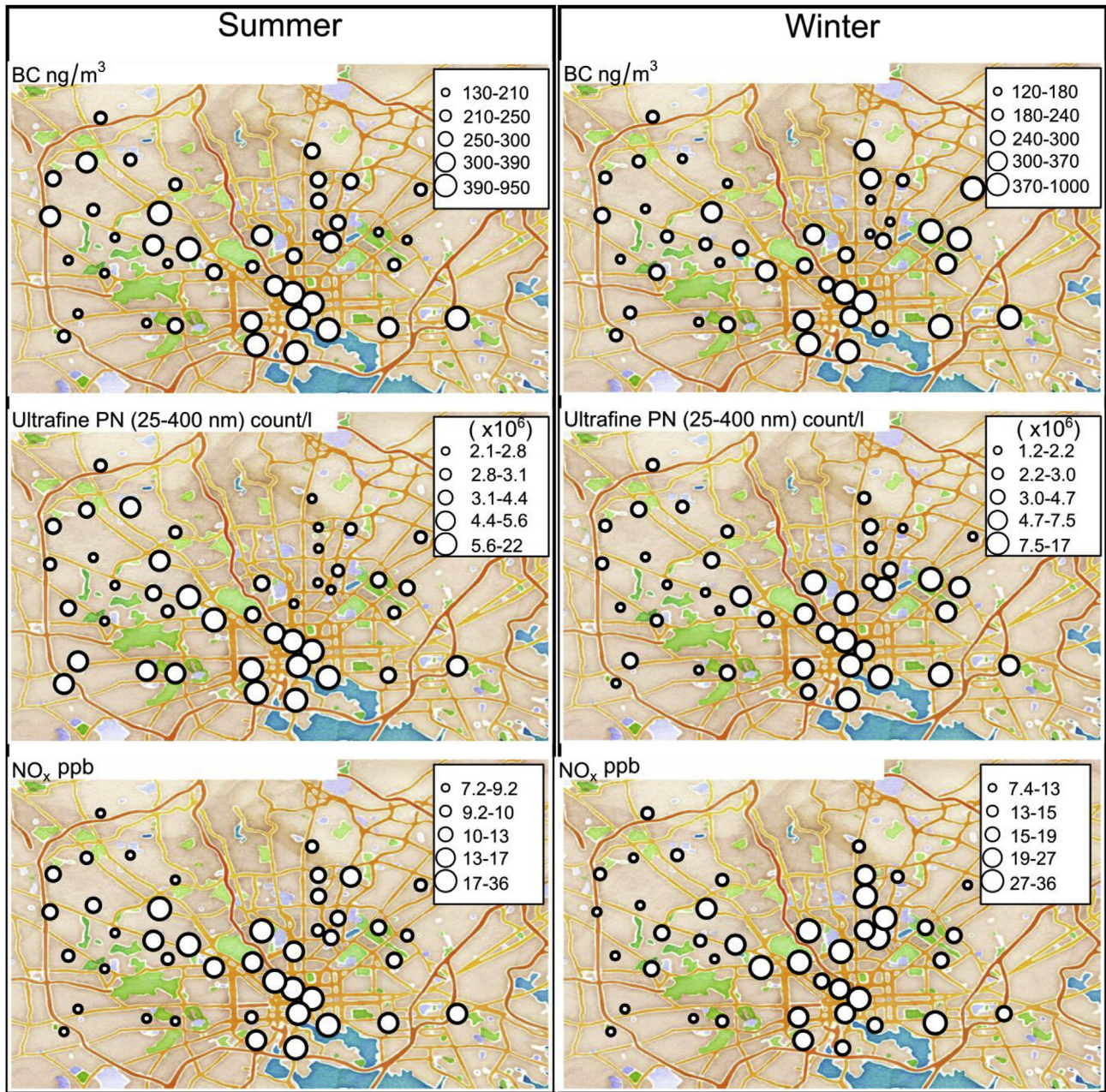


Fig. 2. Spatial distribution of pollutant quintiles for the mobile platform medians after data adjustment (concentrations represent the difference between the measured concentrations and the daily 5th percentile). Maps are a watercolor depiction of Baltimore, MD. Maps produced using the OpenStreetMap package in R (Fellows and Stotz, 2013).

(Pattinson et al., 2014; Van den Bossche et al., 2015), trains (Castellini et al., 2014), and cars (Hudda et al., 2014; Pirjola et al., 2004). Mobile platforms can also be mobile labs consisting of trailers equipped with relatively simple portable instrumentation to highly sophisticated mass spectrometers (Massoli et al., 2012; Sun et al., 2012; von der Weiden-Reimüller et al., 2014). Mobile monitoring provides real-time monitoring at a variety of locations, with the accompanying challenge of being temporally limited at any one place. It provides the means to measure air pollutant concentrations with broad spatial coverage using sophisticated equipment that would otherwise be impractical to duplicate in a fixed monitoring campaign.

Sullivan and Pryor (2014) used a combination of mobile monitoring and four continuous fixed site measurements to investigate the spatio-temporal variability of PM_{2.5} within a small urban region

(~12 km). They found mobile monitoring provided enhanced spatial density whereas continuous fixed site monitors provided temporally-rich data (Sullivan and Pryor, 2014). Other small spatial scale campaigns for black carbon and ultrafine particle counts have shown correlations between mobile routes in proximity to fixed sampling locations (Van den Bossche et al., 2015; Wu et al., 2015). All of these campaigns were limited in spatial extent due to the availability of fixed site locations and duplicate instrumentation both of which are logically complicated to overcome. Duplication of instruments is resource intensive, which also restricts the number of pollutants measured and the ability to study pollutant mixtures.

In this work, we investigate the utility of combining readily deployed PSD and mobile monitoring. PSDs provide wide-spread spatial coverage for a dozen gaseous pollutants and mobile

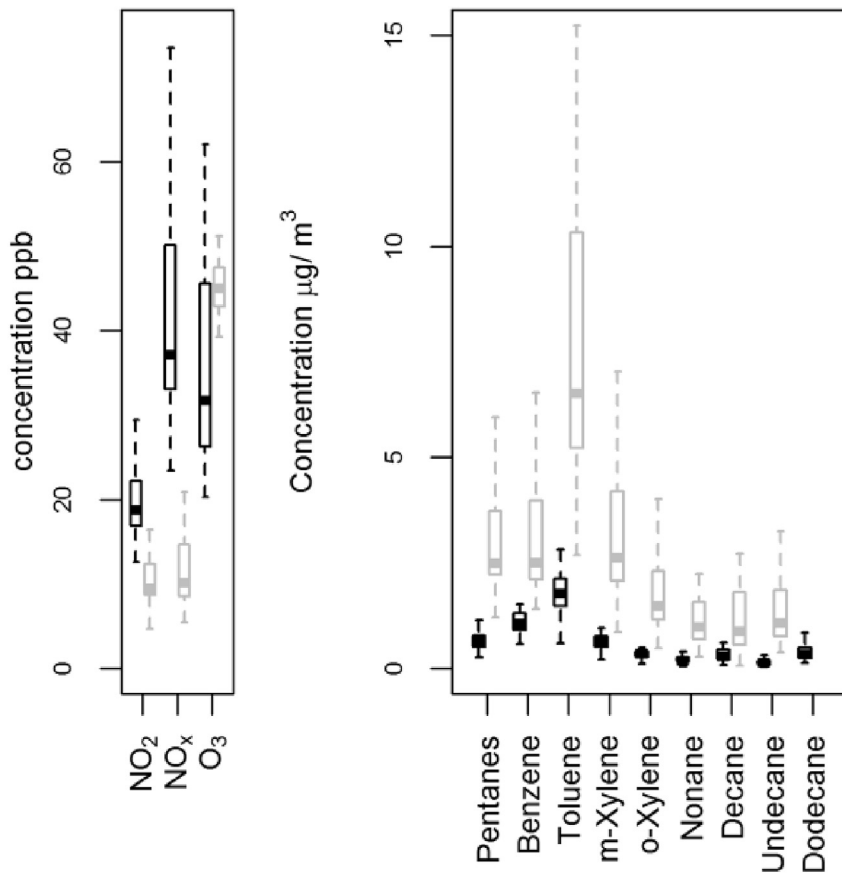


Fig. 3. PSD summaries by analyte. Black (winter) and gray (summer). Pentanes are divided by 100 and include both pentanes and hexanes. For comparison AQS measurements taken in downtown Baltimore (GPS 39.298056, -76.604722) for NO_x averaged 16.7 ppb in summer and 44.6 ppb in the winter over the same time period ([U.S. Environmental Protection Agency Air Quality System \(AQS\) Data Mart, 2012](#)). VOC data collected at the same location for the PAMS monitoring network indicates higher values in the winter rather than the summer for similar compounds. Benzene: 0.18 ppb summer (0.58 µg/m³), 0.37 ppb (1.18 µg/m³) winter. o-Xylene: 0.07 ppb summer (0.3 µg/m³), 0.06 ppb winter (0.26 µg/m³). Hexanes: 0.01 ppb summer (0.035 µg/m³), 0.33 ppb winter (1.16 µg/m³). AQS and PAMS data converted to µg/m³ assume standard temperature and pressure.

monitoring provides complimentary short-term measurements of both gaseous and particulate pollutants. Correlations between PSD and collocated continuous read measurements have been reported by Beckerman et al. in a previous near-roadway gradient study that consisted of a one week deployment of PSDs in Toronto, Canada ([Beckerman et al., 2008](#)). In our study, the sampling design consisted of mobile monitoring of eight pollutants in combination with 2-week fixed-site passive sampling of a combination of nine volatile organic compounds (VOCs), NO₂, NO_x, and ozone. The VOC speciation provided by the passive samplers allows differential detection of light duty (low molecular weight hydrocarbons) and heavy duty vehicles (long-chain alkanes) at each sampling location. In this study we selected forty-three monitoring locations in an approximately 400 km² region encompassing the city and suburbs of Baltimore, MD making this one of the largest mobile monitoring campaigns in terms of spatial extent. Locations were selected to optimize spatial coverage near residences of participants in the Multi-Ethnic Study of Atherosclerosis ([Cohen et al., 2009](#)). Our two monitoring campaigns took place in February (winter) and June (summer) of 2012 to capture seasonal differences in pollutant distributions. We investigate both the pair-wise and multipollutant correlations between the two-week integrated PSD data and the 10-sec average mobile monitoring data in these two seasons.

2. Methods

A detailed description of the methods for sample collection,

sample analysis and statistical treatment of the data is provided in the supplementary material. In brief, two sampling campaigns were conducted in 2012 between February 12–22, 2012 and June 18–27, 2012. The roadway intersections we selected throughout the urban area are depicted in [Fig. 1](#), representing a combination of residential streets and arterials with mixed traffic composition. PSDs positioned on utility poles near the intersections provided two-week integrated measures of various VOCs, ozone, NO_x and NO₂ as listed in [Table 1](#). The PSD data were complemented by measurements obtained from a mobile platform ([Riley et al., 2014](#)) between the hours of 14:00–19:00 local time. Intersections were sampled along fixed routes every third day for a total of ~6–10 min at a sampling rate of 10 s. Each site was sampled 3–4 times during the summer and winter campaigns, and the order of the sampling was reversed each time the route was repeated. We performed mobile monitoring continuously on the move (~20–35 km/h), with each intersection and its surrounding area sampled in an alternating clover leaf pattern ([Larson et al., 2009](#)). We therefore use the term ‘roadway intersection’ to include an area several hundred meters in extent centered on a given intersection. Our mobile monitoring method therefore captures a distribution of air pollution concentrations at each intersection ([Larson et al., 2009](#)). The species used in this analysis are listed in [Table 1](#) and the corresponding mobile instruments and their reporting ranges are provided in [Table S1](#).

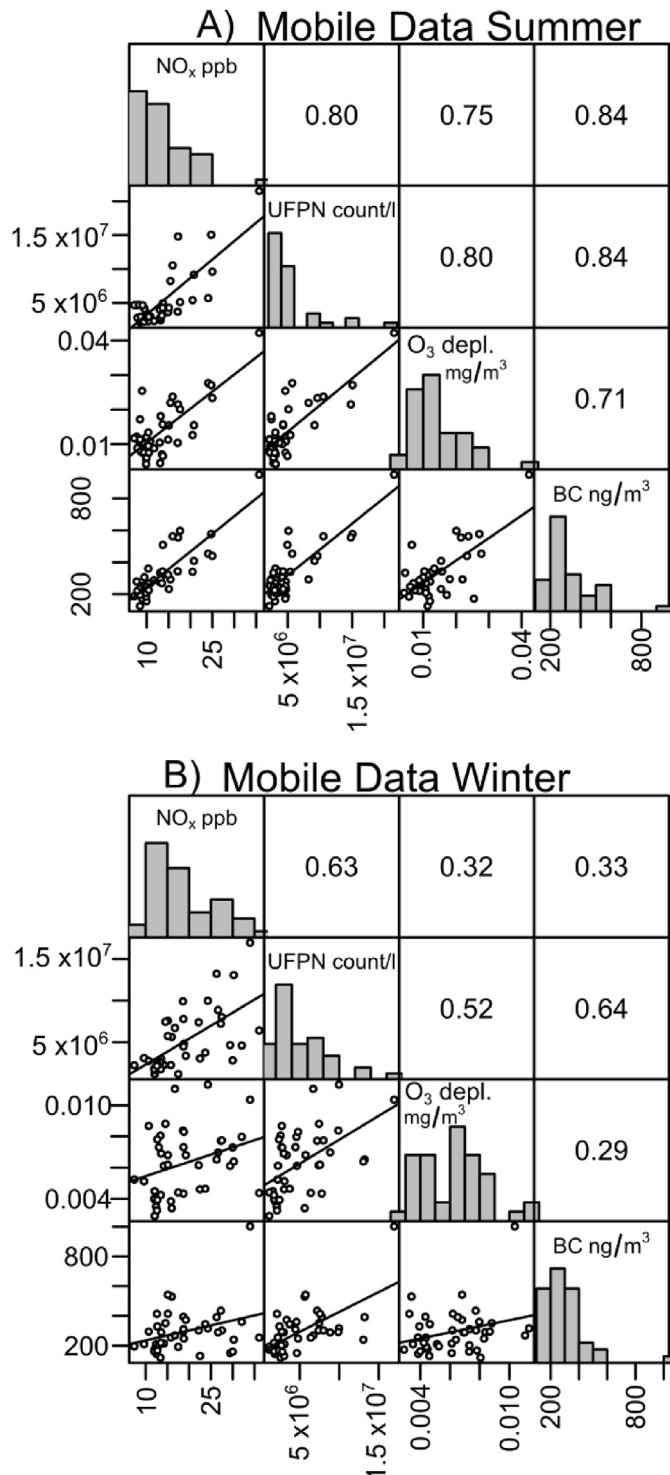


Fig. 4. Correlation scatterplot matrix for select mobile platform species for (A) summer and (B) winter. Pearson's correlation coefficients are in the upper diagonal, values greater than 0.4 are significant (2-sided $p = 0.01$). Each data point represents the median derived from the sampling intersections. Concentrations represent the difference between the measured concentrations and the daily 5th percentile.

2.1. Mobile platform temporal adjustments

A central challenge to the use of mobile monitoring data for spatial analysis is developing methods to adjust for temporally-varying contributions to the observed values, such as day to day

Table 2
Mobile platform Pearson's correlation coefficients, summer.

	UFPN	PN ₁	PN _{Fine}	PN _(1–3μm)	BC	NO _x mob.	CO	O ₃ depl.
UFPN	0.94	0.77	0.82	0.84	0.8	0.33	0.8	
PN ₁	0.94	0.72	0.8	0.84	0.86	0.28	0.78	
PN _{Fine}	0.77	0.72	0.84	0.74	0.59	0.25	0.75	
PN _(1–3μm)	0.82	0.8	0.84	0.76	0.73	0.39	0.78	
BC	0.84	0.84	0.74	0.76		0.84	0.47	0.71
NO _x mob.	0.8	0.86	0.59	0.73	0.84		0.5	0.75
CO	0.33	0.28	0.25	0.39	0.47	0.5		0.42
O ₃ depl.	0.8	0.78	0.75	0.78	0.71	0.75		0.42
VOC	0.52	0.48	0.44	0.57	0.52	0.47	0.49	0.43

The 2 sided probability $p = 0.01$ critical value for Pearson's correlation coefficients is 0.40 for $N = 40$, significant p-values are indicated by bold text. The correlations coefficients are calculated using the medians derived for each sampling intersection after temporal adjustment as described in Section 2.1.

Table 3
Mobile platform Pearson's correlation coefficients, winter.

	UFPN	PN ₁	PN _{Fine}	PN _(1–3μm)	BC	NO _x mob.	O ₃ depl.	
UFPN	0.9	0.6	0.67	0.64	0.63	0.52		
PN ₁	0.9		0.56	0.7	0.73	0.62	0.46	
PN _{Fine}	0.6		0.84		0.76	0.29	0.38	
PN _(1–3μm)	0.67	0.7	0.84		0.88	0.41	0.3	
BC	0.64	0.73	0.76	0.88		0.33	0.29	
NO _x mob.	0.63	0.62	0.29	0.41		0.33	0.32	
O ₃ depl.	0.52	0.46	0.38	0.3		0.29	0.32	
VOC	-0.089	-0.12	-0.049	-0.22		-0.16	-0.096	0.0061

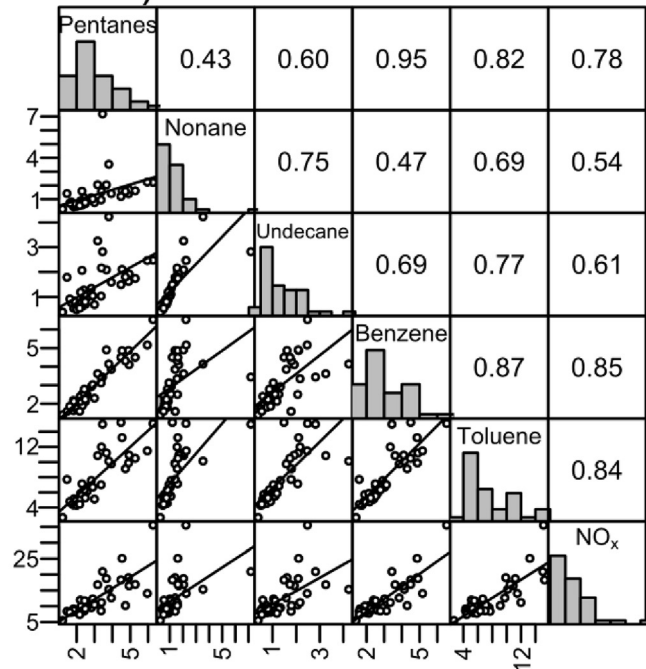
The 2 sided probability $p = 0.01$ critical value for Pearson's correlation coefficients is 0.40 for $N = 40$, significant p-values are indicated by bold text. The correlations coefficients are calculated using the medians derived for each sampling intersection after temporal adjustment as described in Section 2.1.

differences in meteorology that affect the entire region. For this analysis we are interested in determining how much each intersection typically differs from the well-mixed regional background levels as measured by the mobile platform during the study duration. Therefore, we processed the majority of mobile data to adjust for between-day temporal trends by subtracting the daily 5th percentile as discussed in the supplemental information section S4.2.

Mobile ozone measurements and PN_{Fine} ($0.25\text{--}1\text{ }\mu\text{m}$) contained within-day variability due to regional concentration changes (Supplemental S4.2.2 –S4.2.3). Thus we adjusted ozone and PN_{Fine} measurements by subtracting a 30-min rolling 5th percentile (95th percentile for ozone), resulting in variables that are considered localized. The 30-min window ensured that an area ($\sim 6\text{ km}^2$) larger than a single intersection ($\sim 0.36\text{ km}^2$) was used to estimate the background and the 5th percentile is reliably calculated from ~ 180 data points. We refer to the adjusted ozone concentrations as "ozone depletion".

We then aggregated the adjusted mobile data at each roadway intersection across days within season, and calculated the median for each pollutant at each intersection. The median is obviously less sensitive than the mean to the presence of discrete high concentration plumes in the distribution of concentrations measured at an intersection (Riley et al., 2014). The resultant medians are differential concentrations from the estimated daily or 30-min rolling 5th percentile background concentrations. Therefore, a near zero or negative value is interpreted as an intersection whose measured concentrations were among the lowest recorded along each route. Figs. S1 and S2 show that the distributions of concentrations recorded for the different routes were not systematically different from one another.

A) PSD Data Summer



B) PSD Data Winter

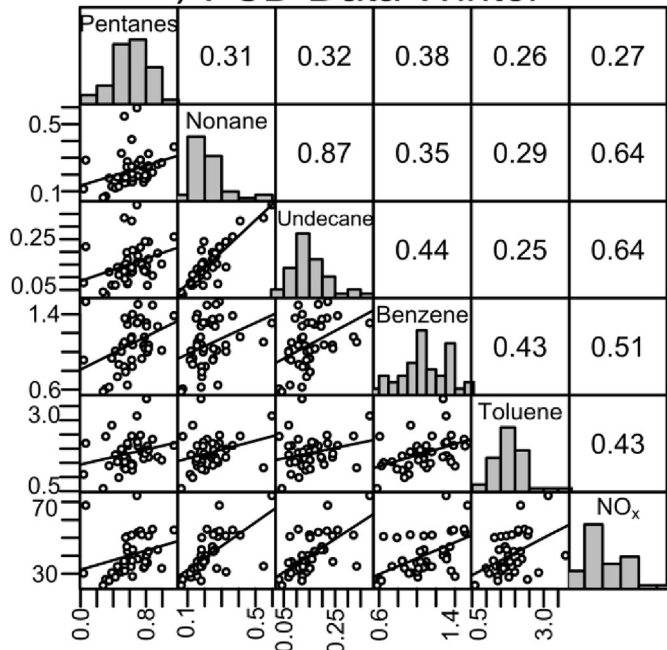


Fig. 5. Correlation scatterplot matrix for select passive sampler detector species for (A) summer and (B) winter. Pearson's correlation coefficients are in the upper diagonal, values greater than 0.4 are significant (2-sided $p = 0.01$). Organic species have units of $\mu\text{g}/\text{m}^3$, Pentanes have been divided by a factor of 100, and NO_x has units of ppb.

2.2. Mobile and PSD measurement correlations

Mobile data was then merged with the PSD data to generate the analysis dataset for each season. The resulting data files are available in the supplemental information. We calculated the Pearson's correlation coefficients for the mobile data medians and the corresponding PSD 2-week averages, separately for each season. Because the PSD ozone measurements were uncorrelated with

other pollutants we excluded them from the principal component analysis (PCA). We standardized the data by mean-centering and scaling by the variance, and calculated principal components from the correlation matrix using the function 'principal' from the R package "psych" (Revelle, 2015). We determined the number of components selected by requiring eigenvalues to be greater than one. To aid in interpretability of the components, we then rotated the selected components using Varimax.

3. Results

3.1. Study area description

A map of the roadway intersections is provided in Fig. 1. The map includes annual average weekday traffic counts, and train traffic routes. Environmentally critical areas of the sampling region include a 1 km perimeter along the port, where sites 1 to 5 and site 43 are located. The port is serviced by a large number of low-traffic roads with high percentages of diesel truck traffic (truck traffic counts not shown). The roadway intersections are divided among the three different sampling routes; roadway intersection sites along the same route share common color shading.

3.2. Mobile data adjustments

Boxplots of the distribution of 10 s measurements taken at the roadway intersections are provided in the supplemental information (Figs. S8–16) for both the unadjusted data as well as the adjusted data. The adjusted data were used to calculate the medians for each species at the roadway intersections for the two-week period, and the medians are indicated by the black dashed line in the figures. Black carbon (BC), ozone depletion, ultrafine particle number count (UFPN), and NO_x all exhibit cross-season similarities in which specific roadway intersections had elevated concentrations of the respective species; for example, intersections in the downtown region are consistently elevated for pollutant concentrations as compared to the rest of the city. The spatial pattern is evident in the maps of the quintiles of the median concentrations for mobile species NO_x, BC, and UFPN after data adjustment (Fig. 2). The winter campaign took place during stronger winds than in summer with most days exhibiting a westerly direction (see Figs. S17 and S18); this may account for higher concentrations of BC and UFPN on the eastern side of the city relative to summer which had no prevailing wind direction and lower wind speeds.

3.3. PSD summary statistics

Boxplots for the PSD data are provided in Fig. 3. The summer campaign had higher concentrations of each VOC species compared to the winter campaign (dodecane was excluded from the summer data due to high limit of detection from laboratory contamination). Both seasons exhibit a similar ranking of VOC concentrations: low molecular weight hydrocarbons had higher concentrations than the long chain alkanes ($>\text{C}6$). Ozone concentrations were highest in the summer; conversely, oxides of nitrogen were higher in the winter consistent with observations at a nearby AQS monitor (see caption to Fig. 3). The mobile monitoring platform also measured higher VOC and NO_x concentrations in the summer compared to winter (see unadjusted data in the SI).

3.4. Mobile platform correlations

Scatterplot matrices for a subset of air pollutants measured by the mobile platform are presented in Fig. 4 for summer and winter.

Table 4

PSD Pearson's correlation coefficients, summer.

	Pentanes	Benzene	Toluene	<i>m</i> -Xylene	<i>o</i> -Xylene	Nonane	Decane	Undecane	NO ₂	NO _x
Pentanes		0.95	0.82	0.79	0.76	0.43	0.48	0.6	0.73	0.78
Benzene	0.95		0.87	0.86	0.84	0.47	0.59	0.69	0.81	0.85
Toluene	0.82	0.87		0.98	0.94	0.69	0.58	0.77	0.8	0.84
<i>m</i> -Xylene	0.79	0.86	0.98		0.97	0.62	0.58	0.76	0.78	0.83
<i>o</i> -Xylene	0.76	0.84	0.94	0.97		0.65	0.72	0.85	0.75	0.8
Nonane	0.43	0.47	0.69	0.62	0.65		0.61	0.75	0.54	0.54
Decane	0.48	0.59	0.58	0.58	0.72	0.61		0.91	0.48	0.47
Undecane	0.6	0.69	0.77	0.76	0.85	0.75	0.91		0.62	0.61
NO ₂	0.73	0.81	0.8	0.78	0.75	0.54	0.48	0.62		0.96
NO _x	0.78	0.85	0.84	0.83	0.8	0.54	0.47	0.61	0.96	
O ₃	0.39	0.44	0.25	0.24	0.23	0.024	0.17	0.16	0.45	0.46

The 2 sided probability p = 0.01 critical value for Pearson's correlation coefficients is 0.40 for N = 40, significant p-values are indicated by bold text.

Table 5

PSD Pearson's correlation coefficients, winter.

	Pentanes	Benzene	Toluene	<i>m</i> -Xylene	<i>o</i> -Xylene	Nonane	Decane	Undecane	Dodecane	NO ₂	NO _x
Pentanes		0.38	0.26	0.44	0.45	0.31	0.054	0.32	0.022	0.084	0.27
Benzene	0.38		0.43	0.47	0.46	0.35	0.22	0.44	0.15	0.43	0.51
Toluene	0.26	0.43		0.51	0.5	0.29	-0.004	0.25	-0.061	0.19	0.43
<i>m</i> -Xylene	0.44	0.47	0.51		0.99	0.76	0.39	0.74	0.3	0.49	0.79
<i>o</i> -Xylene	0.45	0.46	0.5	0.99		0.78	0.38	0.75	0.29	0.49	0.79
Nonane	0.31	0.35	0.29	0.76	0.78		0.48	0.87	0.32	0.5	0.64
Decane	0.054	0.22	-0.004	0.39	0.38	0.48		0.65	0.93	0.22	0.22
Undecane	0.32	0.44	0.25	0.74	0.75	0.87	0.65		0.46	0.63	0.64
Dodecane	0.022	0.15	-0.061	0.3	0.29	0.32	0.93	0.46		0.068	0.12
NO ₂	0.084	0.43	0.19	0.49	0.49	0.5	0.22	0.63	0.068		0.76
NO _x	0.27	0.51	0.43	0.79	0.79	0.64	0.22	0.64	0.12	0.76	
O ₃	0.1	0.28	0.27	0.077	0.065	-0.1	0.039	-0.13	0.2	0.014	0.2

The 2 sided probability p = 0.01 critical value for Pearson's correlation coefficients is 0.40 for N = 40, significant p-values are indicated by bold text.

Histograms of concentrations show a tendency toward lower concentrations. The scatterplots generally follow a linear relationship in the summer, but a similarly clear trend is not evident in the winter. The correlation coefficients for the entire mobile dataset are provided in Tables 2 and 3 for summer and winter, respectively. Correlations are strongest between the particulate matter pollutants, and are stronger overall in the summer.

3.5. PSD correlations

Scatterplot matrices for the subset of air pollutants measured by the PSDs are presented in Fig. 5 for summer and winter. The summer scatterplots follow the linear regression line reasonably well, but this is not observed in the winter except for a few cases (nonane and undecane). Histograms of PSD concentrations appear to be less skewed toward lower concentrations than those for the mobile platform data (Fig. 4). The correlation coefficients for the entire PSD dataset are provided in Tables 4 and 5 for summer and winter respectively. The pollutants measured in summer were all significantly correlated ($p = 0.01$) except for PSD ozone. Correlations are weaker in the winter, and less than half of them are significant at $p = 0.01$.

3.6. PSD vs. mobile correlations

Scatterplot matrices between a subset of mobile monitoring medians and PSD data are provided in Fig. 6. The scatterplots generally follow a linear regression for the summer campaign, but again not for the winter campaign. The correlation coefficients between the entire PSD and Mobile datasets are provided in Tables 6 and 7. The correlation matrix for summer reveals some high correlations between mobile platform and PSD data. In particular, CO has a higher correlation with PSD pentanes than it

does with any other mobile platform measurements which is also observed in the scatterplots. PSD NO_x is highly correlated to mobile NO_x and also with BC, UFPN and ozone depletion. Ozone depletion is moderately correlated with PSD ozone as is mobile NO_x. No other correlations are significant for PSD ozone in summer. The summer exhibited significant correlations between all mobile platform and PSD compounds except for PSD decane and ozone. In contrast, the majority of correlations observed in the winter between PSD and mobile data are insignificant (at $p = 0.01$). For seven of the monitoring days in winter, precipitation was recorded in the form of rain, snow, or fog. Winter wind speed averages exceeded 7 mph on 7 of the monitoring days with higher gusts (see Figs. S17–18). These meteorological factors may have resulted in increased deposition and dispersion of pollutants.

The effect of the choice of temporal data adjustments on the correlation coefficients is presented in Section S5.2 in the supplemental materials. We find that the daily 5th percentile adjustment gave the highest correlation between PSD and mobile data except for PN_{fine} and ozone for which the rolling 30-min 5th and 95th percentile adjustments (respectively) resulted in the highest correlations.

3.7. Principal component analysis

The rotated principal components (RC) are compared between PSD only data and combined PSD and mobile platform data in Fig. 7 for the summer season only, where correlations between pollutants were strongest. Winter RCs were similar to the features derived for the summer dataset although they were not directly comparable due to the absence of mobile CO in the winter and dodecane in the summer. We excluded winter data from this analysis because bootstrap resampling of the winter data revealed that the RCs derived were unstable.

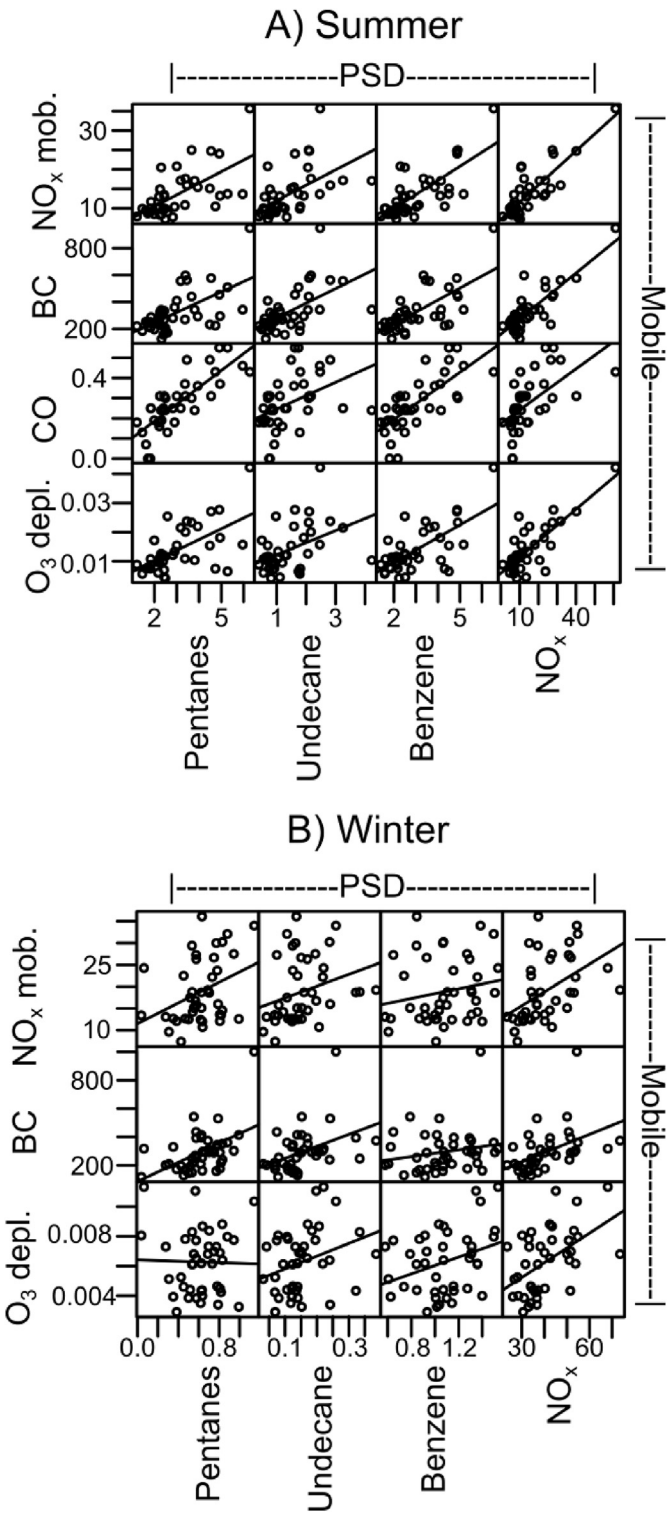


Fig. 6. Scatterplot matrix comparing select mobile platform and PSD species concentrations (units provided in Table 1).

The PSD data yield two components that explain 87% of the total variability. One RC consists of high loadings for low molecular weight hydrocarbons, NO₂, NO_x, and the other RC has high loadings of long chain alkanes. Adding the mobile platform data results in three components with 83% of the total variance explained. Adding the mobile data further parses the low molecular weight VOC and

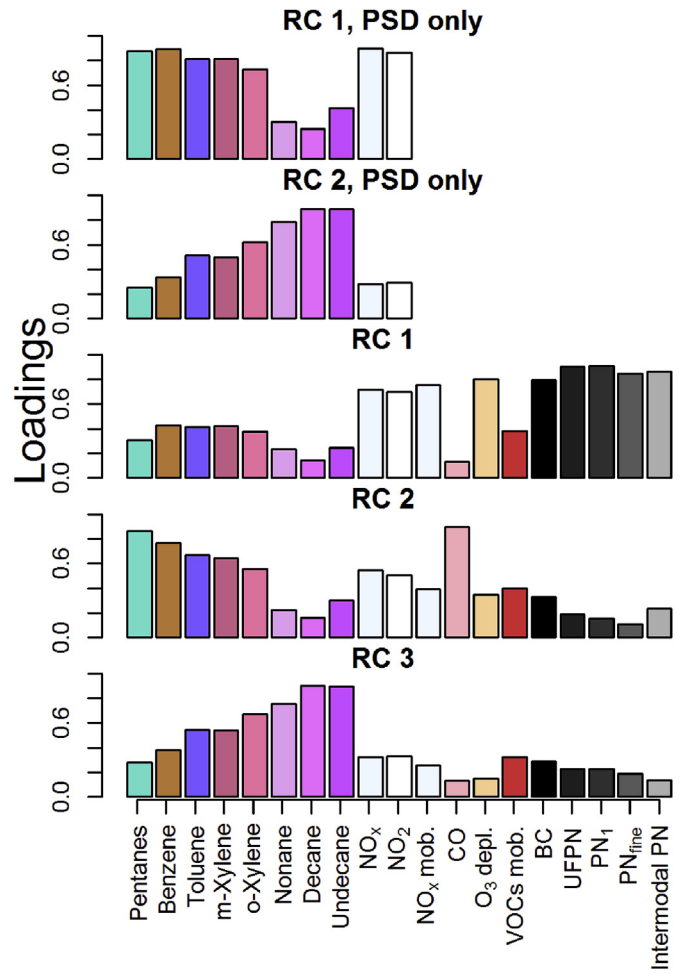


Fig. 7. Summer season principal component analyses with varimax rotation for PSD data and the combined mobile medians and PSD data, respectively. Loadings of rotated components (RC) are depicted. Breakdown of variance explained PSD only: RC1_{PSD} 53% and RC2_{PSD} 34%. Combined mobile and PSD: RC1 37%, RC2 25% and RC3 22% (Total 83%).

NO_x PSD data into two components instead of one. The correlations we observed between the mobile data and the PSD data are also evident in the first two components of the combined data analysis. In the combined dataset the first component has high loadings for particle counts, NO_x mobile, and ozone depletion and PSD NO_x and NO₂, whereas the second component consists of CO highly correlated with low molecular weight hydrocarbons. The third component appears to be long chain VOCs that had little correlation to low molecular weight VOCs and the mobile data.

4. Discussion

Whether or not short-term mobile monitoring data are representative of longer-term (2-week) measurements greatly impacts the utility of mobile monitoring campaigns in characterizing spatial patterns in air pollution. The first challenge in comparing mobile monitoring and PSD datasets is to define an appropriate measure of central tendency for the mobile monitoring species at each of the intersections, across the days of sampling. Our sampling scheme makes repeat measurements at roadway intersections every third day for a total of 3–4 visits lasting 6–10 min each. The distributions of measurements at a given intersection made on these separate days could differ depending upon temporally-varying factors such as traffic characteristics (weekend/weekday), meteorological

Table 6

PSD vs. Mobile Pearson's Correlation Coefficients, Summer.

	UFPN	PN ₁	PN _{Fine}	PN _(1–3μm)	BC	NO _x mob.	CO	O ₃ depl.	VOC
Pentanes	0.51	0.47	0.44	0.49	0.61	0.63	0.81	0.6	0.57
Benzene	0.62	0.6	0.51	0.58	0.7	0.74	0.73	0.67	0.54
Toluene	0.62	0.6	0.55	0.6	0.69	0.67	0.7	0.66	0.57
<i>m</i> -Xylene	0.62	0.61	0.54	0.61	0.67	0.67	0.65	0.65	0.53
<i>o</i> -Xylene	0.58	0.59	0.52	0.56	0.64	0.66	0.58	0.6	0.5
Nonane	0.42	0.38	0.44	0.36	0.5	0.38	0.46	0.4	0.42
Decane	0.36	0.37	0.27	0.29	0.41	0.48	0.27	0.31	0.39
Undecane	0.5	0.47	0.39	0.41	0.58	0.55	0.42	0.44	0.53
NO ₂	0.79	0.77	0.69	0.71	0.83	0.83	0.58	0.77	0.44
NO _x	0.82	0.8	0.71	0.73	0.83	0.84	0.59	0.8	0.51
O ₃	0.38	0.37	0.33	0.28	0.39	0.49	0.32	0.55	-0.081

The 2 sided probability $p = 0.01$ critical value for Pearson's correlation coefficients is 0.40 for $N = 40$, significant p-values are indicated by bold text. The correlations coefficients are calculated between the PSD data and the medians derived for each sampling intersection after temporal adjustment of the mobile platform data as described in Section 2.1.

factors (mixing height and wind speed and direction), and time of sampling (mid-afternoon versus evening/sundown). In this paper we chose to adjust the distributions to minimize between-day temporal variations in order to allow all other sources of variability to be aggregated over multiple days of sampling. Median values for each pollutant at each intersection were obtained from these aggregated distributions. Mobile platform measurements of absolute ozone concentration and absolute PN_{fine} were excluded from this analysis because within-day variability due to meteorological or other non-local factors (regional transport) dominates the variability for these metrics (Wu et al., 2015; Yli-Tuomi et al., 2005). For example, the boxplots for unadjusted PN_{fine} and ozone concentrations (Figs. S15–S16) compared to unadjusted BC (Fig. S14) indicate that ozone concentrations are affected by both within and between day factors as evidenced by large daily concentration changes and vastly differing daily spatial patterns. In contrast, consistent spatial patterns are observed in the quintiles of UFPN, BC, and NO_x following data adjustment (see Fig. 2). This choice of data adjustment is discussed in further detail in supplemental S4.2.

The VOCs measured on the PSD in winter were overall much lower in concentration than in the summer; however, the relative concentrations of the pollutants measured were similar in the two seasons indicating some consistency in the measurements. The Photochemical Assessment Monitoring Station (PAMS) data for Baltimore, which is located at the downtown AQS site, measured higher VOC concentrations in winter, and the concentrations were overall lower than what we measured on the PSDs. The PAMS data consists of one 24 h sample every 6th day and therefore does not provide a direct comparison. The variability in concentrations

observed in winter is lower, which may account for the weaker correlations between VOCs in this season. PSD NO_x and NO₂ exhibit seasonal differences as well. In the summer, NO_x and NO₂ have nearly identical distributions of concentrations (see Fig. 2) and are correlated with $r = 0.96$, whereas in winter, NO_x is almost twice the concentration of NO₂ and the correlation is $r = 0.76$. This indicates that NO_x in summer is almost entirely NO₂, whereas in winter NO makes up a substantial amount of NO_x concentrations.

The only pollutant common to both the PSD and mobile monitoring sampling was NO_x, and the scatterplot matrices in Fig. 6 illustrate that the mobile monitoring and PSD measures were correlated for this pollutant, especially during the summer campaign. This result indicates that source activity that was sampled briefly by mobile monitoring in four afternoon visits distributed across two weeks is relevant to the source activity sampled over the entire two weeks. The strong correlation between PSD pentanes and mobile CO in the summer campaign is particularly noteworthy because these combined measurements indicate that the sampling strategy is detecting VOCs arising from mobile sources (in US cities ~95% of CO is emitted from vehicles) (U.S. EPA, 2008). The presence of significant correlation between the PSDs and adjusted mobile platform measurements suggests that the comparatively limited amount of time sampling at each site by the mobile platform averaged across multiple visits is in fact representative of longer-term spatial contrasts between locations within a city (Fig. 2). This observation is particularly helpful for interpreting particle count distributions as well as BC measurements for which there so far have been few low-cost solutions for obtaining multiple, simultaneous, fixed site, time-integrated measurements.

Table 7

PSD vs. Mobile Pearson Correlation Coefficients, Winter.

	UFPN	PN ₁	PN _{Fine}	PN _(1–3μm)	BC	NO _x mob.	O ₃ depl.	VOC
Pentanes	0.32	0.43	0.21	0.41	0.49	0.36	-0.024	-0.04
Benzene	0.3	0.23	0.16	0.12	0.19	0.19	0.33	0.22
Toluene	0.071	0.074	-0.034	0.074	0.095	0.031	-0.14	0.12
<i>m</i> -Xylene	0.45	0.48	0.33	0.36	0.45	0.32	0.19	0.18
<i>o</i> -Xylene	0.42	0.45	0.33	0.36	0.44	0.3	0.19	0.18
Nonane	0.42	0.45	0.32	0.29	0.37	0.31	0.25	0.17
Decane	0.22	0.18	0.18	0.12	0.23	0.021	0.13	0.13
Undecane	0.48	0.47	0.48	0.38	0.42	0.28	0.31	0.26
Dodecane	0.064	0.064	0.078	0.035	0.15	-0.062	0.083	0.096
NO ₂	0.6	0.51	0.53	0.43	0.38	0.39	0.48	0.3
NO _x	0.6	0.53	0.47	0.44	0.47	0.48	0.51	0.2
O ₃	-0.2	-0.19	-0.064	-0.08	0.073	-0.18	0.13	0.08

The 2 sided probability $p = 0.01$ critical value for Pearson's correlation coefficients is 0.40 for $N = 40$, significant p-values are indicated by bold text. The correlations coefficients are calculated between the PSD data and the medians derived for each sampling intersection after temporal adjustment of the mobile platform data as described in Section 2.1.

The correlation results (especially from summer) are consistent with previous campaigns comparing mobile data to fixed site and near roadway monitors. Typically it is found that the mobile platform concentrations are most correlated with the fixed site measurements collected nearest to the mobile route (Sullivan and Pryor, 2014; Van den Bossche et al., 2015). Beckerman et al. reported correlations between continuous measurements (ultrafine particle mass and PM_{2.5}) and 1 week PSD (Ogawa and 3 M) measurements of NO₂, NO_x, ozone, benzene, xylenes, and hexanes (among other VOCs) in a colocation experiment measuring the near road gradient of two major highways (Beckerman et al., 2008). They report similar correlation coefficients to our summer campaign (between 0.6 and 0.8), although they have fewer points of comparison and their monitor placements were measuring the same source. Our correlations between UFPN and VOCs are also similar to those reported from a near-roadway gradient measurement made by real-time instruments in a summer campaign in Raleigh, North Carolina (Hagler et al., 2009). Correlations between pollutants on mobile platforms have also been found to vary by neighborhood in some studies with correlation coefficients ranging between 0.35 and 0.8 between particle number counts and NO_x (Patton et al., 2014), which may indicate variation in traffic characteristics.

The principal components analysis on the PSD-only data resulted in two components compared to three for the combined PSD and mobile analysis for the summer. The PSD-only rotated components reveal that the majority of the variance is described by a feature enriched in low molecular weight hydrocarbons and NO_x. However, with the addition of the mobile platform measurements, the VOC and NO_x data are split among three features. The strong correlations between the PSD NO_x measures and the mobile platform NO_x, BC, and particulate matter species are revealed in the first component. Whereas the strong correlations between mobile CO and the low molecular weight hydrocarbons appear in the second feature. Finally, the least amount of variance is attributed to the high molecular weight hydrocarbon feature, RC3. Our findings are similar to Oakes and colleagues, who found that NO_x was approximately evenly split between multipollutant features they designated as diesel, gasoline, and “total mobile sources” (Oakes et al., 2014). RC1 for the combined data has loadings consistent with emission factors for diesel exhaust (Hudda et al., 2013; Westerdahl et al., 2005). RC2 has high loadings of mobile CO and lower molecular weight hydrocarbons as well as mobile and PSD NO_x; this feature is consistent with light duty vehicle traffic (Hudda et al., 2013; Oakes et al., 2014). Finally, RC3 is enhanced in the longer chain alkanes ($n > 6$) that are uncorrelated with both PN and BC concentrations, typical of uncontrolled crankcase emissions from diesel engine road-draft tubes (Zielinska et al., 2008).

This work only used afternoon mobile sampling measurements, which is a potential limitation of this study particularly in winter when 1–3 h of sampling occurs after dark. Also the PSD samplers capture the morning commute in addition to the afternoon commute, which might also be an important factor for correlations between PSD and mobile measurements in winter. In summer, we note, that correlations between PSD and mobile measurements exceed 0.8 which indicates the mobile platform sampling strategy is capturing the spatial variability in this season. In summer, the absence of a prevailing wind direction over the duration of the two-week period was serendipitous as the concentrations at intersections near highways would ordinarily be impacted by downwind transport. The weaker correlations in winter (including PSD only) were unexpected since winter typically exhibits stronger correlations between air pollutants as has been reported by Patton et al. (2014). Typically higher correlations in winter have been attributed to increased atmospheric stability. We speculate several days of precipitation and strong winds during the winter campaign

may have contributed to the weaker correlations for both PSD and mobile measurements. Therefore, the generalizability of the correlation results for the two week period of the campaign to the remainder of winter is questionable.

5. Conclusions

We have presented an analysis of the correlations between long-term integrated PSD data and short-term, time resolved mobile monitoring data. The correlations we observed between the PSD and mobile measurements demonstrated that underlying spatial variability in specific TRAP components could be reliably captured in a relatively short total measurement time at each location, provided those measurements were aggregated over several days, and that the data are appropriately adjusted for between day changes in background concentrations of each component. This is particularly helpful in that several of the pollutants monitored with the mobile platform (e.g. BC, PN₁) cannot be measured with inexpensive PSDs. In addition, for pollutants where regional transport dominates the variance in concentrations (ozone and PM_{2.5}), a 30-min moving 5th percentile (or 95th percentile for ozone) sufficiently isolates the local contribution to observed concentrations.

It is not straightforward to adjust for confounding temporal factors in a spatially and temporally varying dataset. For interested readers, we've included a more detailed discussion of how the correlation results change with choice of temporal correction in the supplement Section S.5.2. Finally, a PCA of the combined PSD and mobile monitoring data revealed a number of multipollutant mixtures, and these features were more consistent with published source profiles for TRAP, compared to an analysis based on the PSD data alone.

Acknowledgements

This publication was made possible by USEPA grant (RD-83479601-0). Its contents are solely the responsibility of the grantee and do not necessarily represent the official views of the USEPA. Further, USEPA does not endorse the purchase of any commercial products or services mentioned in the publication. Additional support provided by the National Institute of Environmental Health Sciences (T32ES015459, P30ES007033). This publication's contents are solely the responsibility of the authors and do not necessarily represent the official views of the sponsoring agencies. Laboratory analysis of the 3M passive sampler detectors was performed by the Environmental Health Laboratory at the University of Washington under direction of Dr. Russell Dills.

Appendix A. Supplementary data

Supplementary data related to this article can be found at <http://dx.doi.org/10.1016/j.atmosenv.2016.03.001>.

References

- Beckerman, B., Jerrett, M., Brook, J.R., Verma, D.K., Arain, M.A., Finkelstein, M.M., 2008. Correlation of nitrogen dioxide with other traffic pollutants near a major expressway. *Atmos. Environ.* 42 (2), 275–290.
- Castellini, S., Moroni, B., Cappelletti, D., 2014. PMetro: measurement of urban aerosols on a mobile platform. *Measurement* 49, 99–106.
- City of Baltimore, Open Baltimore, Shape file Baltimore railroad (2008). <https://data.baltimorecity.gov/browse?category=Geographic>.
- Cohen, M.A., Adar, S.D., Allen, R.W., Avol, E., Curl, C.L., Gould, T., Hardie, D., Ho, A., Kinney, P., Larson, T.V., Sampson, P., Sheppard, L., Stukovsky, K.D., Swan, S.S., Liu, L.J.S., Kaufman, J.D., 2009. Approach to estimating participant pollutant exposures in the multi-ethnic study of Atherosclerosis and air pollution (MESA air). *Environ. Sci. Technol.* 43 (13), 4687–4693.
- Dons, E., Temmerman, P., Van Poppel, M., Bellemans, T., Wets, G., Panis, L.I., 2013a. Street characteristics and traffic factors determining road users' exposure to

- black carbon. *Sci. Total Environ.* 447, 72–79.
- Dons, E., Van Poppel, M., Kochan, B., Wets, G., Int Panis, L., 2013b. Modeling temporal and spatial variability of traffic-related air pollution: hourly land use regression models for black carbon. *Atmos. Environ.* 74, 237–246.
- ESRI Inc, 2014. ArcGIS: ArcMap, 10.2.2.3552.
- Fellows, I., Stotz, J.P., 2013. OpenStreetMap: Access to Open Street Map Raster Images, 0.3.1.
- Geography Division, U.S. Department of Commerce (U.S. Census Bureau), 2008. TIGER/Line Shapefile county, Baltimore city, MD (24510). <http://www.census.gov/geo/maps-data/data/tiger-line.html>.
- Hagler, G.S.W., Baldauf, R.W., Thoma, E.D., Long, T.R., Snow, R.F., Kinsey, J.S., Oudejans, L., Gullett, B.K., 2009. Ultrafine particles near a major roadway in Raleigh, North Carolina: downwind attenuation and correlation with traffic-related pollutants. *Atmos. Environ.* 43 (6), 1229–1234.
- Hudda, N., Fruin, S., Delfino, R.J., Sioutas, C., 2013. Efficient determination of vehicle emission factors by fuel use category using on-road measurements: downward trends on Los Angeles freight corridor I-710. *Atmos. Chem. Phys.* 13 (1), 347–357.
- Hudda, N., Gould, T., Hartin, K., Larson, T.V., Fruin, S.A., 2014. Emissions from an international airport increase particle number concentrations 4-fold at 10 km downwind. *Environ. Sci. Technol.* 48 (12), 6628–6635.
- Larson, T., Henderson, S.B., Brauer, M., 2009. Mobile monitoring of particle light absorption coefficient in an urban area as a basis for land use regression. *Environ. Sci. Technol.* 43 (13), 4672–4678.
- Marc, M., Zabiegala, B., Namiesnik, J., 2012. Mobile systems (portable, handheld, transportable) for monitoring air pollution. *Crit. Rev. Anal. Chem.* 42 (1), 2–15.
- Massoli, P., Fortner, E.C., Canagaratna, M.R., Williams, L.R., Zhang, Q., Sun, Y., Schwab, J.J., Trimborn, A., Onasch, T.B., Demerjian, K.L., Kolb, C.E., Worsnop, D.R., Jayne, J.T., 2012. Pollution gradients and chemical characterization of particulate matter from vehicular traffic near major roadways: results from the 2009 Queens College Air Quality Study in NYC. *Aerosol Sci. Technol.* 46 (11), 1201–1218.
- Oakes, M.M., Baxter, L.K., Duvall, R.M., Madden, M., Xie, M.J., Hannigan, M.P., Peel, J.L., Pachon, J.E., Balachandran, S., Russell, A., Long, T.C., 2014. Comparing multipollutant emissions-based mobile source indicators to other single pollutant and multipollutant indicators in different urban areas. *Int. J. Env. Res. Public Health* 11 (11), 11727–11752.
- Pattinson, W., Longley, I., Kingham, S., 2014. Using mobile monitoring to visualise diurnal variation of traffic pollutants across two near-highway neighbourhoods. *Atmos. Environ.* 94 (0), 782–792.
- Patton, A.P., Perkins, J., Zamore, W., Levy, J.I., Brugge, D., Durant, J.L., 2014. Spatial and temporal differences in traffic-related air pollution in three urban neighborhoods near an interstate highway. *Atmos. Environ.* 99, 309–321.
- Pirjola, L., Parvainen, H., Hussein, T., Valli, A., Hameri, K., Aalto, P., Virtanen, A., Keskinen, J., Pakkanen, T.A., Makela, T., Hillamo, R.E., 2004. "Sniffer" – a novel tool for chasing vehicles and measuring traffic pollutants. *Atmos. Environ.* 38 (22), 3625–3635.
- Revelle, W., 2015. Psych: Procedures for Personality and Psychological Research, 1.5.6. Northwestern University, Evanston, Illinois, USA.
- Riley, E.A., Banks, L., Fintzi, J., Gould, T.R., Hartin, K., Schaal, L., Davey, M., Sheppard, L., Larson, T., Yost, M.G., Simpson, C.D., 2014. Multi-pollutant mobile platform measurements of air pollutants adjacent to a major roadway. *Atmos. Environ.* 98 (0), 492–499.
- State Highway Administration, Maryland Department of transportation, 2012. Annual Average Daily Traffic Counts. <http://sha.maryland.gov/pages/GIS.aspx?PageID=838>.
- Sullivan, R., Pryor, S., 2014. Quantifying spatiotemporal variability of fine particles in an urban environment using combined fixed and mobile measurements. *Atmos. Environ.* 89, 664–671.
- Sun, Y.L., Zhang, Q., Schwab, J.J., Chen, W.N., Bae, M.S., Hung, H.M., Lin, Y.C., Ng, N.L., Jayne, J., Massoli, P., Williams, L.R., Demerjian, K.L., 2012. Characterization of near-highway submicron aerosols in New York City with a high-resolution aerosol mass spectrometer. *Atmos. Chem. Phys.* 12 (4), 2215–2227.
- U.S. Environmental Protection Agency, Air Quality System Data Mart, 2012. Data for Oldtown Fire Station, 1100 Hillen Street (July 2013). <http://www.epa.gov/tnn/airs/aqsdamart/access/interface.htm>.
- U.S. EPA, 2008. Latest Findings on National Air Quality: Status and Trends through 2006, p. p 22. EPA-454/R-07-007; Research Triangle Park, NC.
- Van den Bossche, J., Peters, J., Verwaeren, J., Botteldooren, D., Theunis, J., De Baets, B., 2015. Mobile monitoring for mapping spatial variation in urban air quality: development and validation of a methodology based on an extensive dataset. *Atmos. Environ.* 105, 148–161.
- von der Weiden-Reinmüller, S.L., Drewnick, F., Zhang, Q.J., Freutel, F., Beekmann, M., Borrmann, S., 2014. Megacity emission plume characteristics in summer and winter investigated by mobile aerosol and trace gas measurements: the Paris metropolitan area. *Atmos. Chem. Phys.* 14 (23), 12931–12950.
- Westerdahl, D., Fruin, S., Sax, T., Fine, P.M., Sioutas, C., 2005. Mobile platform measurements of ultrafine particles and associated pollutant concentrations on freeways and residential streets in Los Angeles. *Atmos. Environ.* 39 (20), 3597–3610.
- Wu, H., Reis, S., Lin, C., Beverland, I.J., Heal, M.R., 2015. Identifying drivers for the intra-urban spatial variability of airborne particulate matter components and their interrelationships. *Atmos. Environ.* 112, 306–316.
- Yli-Tuomi, T., Aarnio, P., Pirjola, L., Makela, T., Hillamo, R., Jantunen, M., 2005. Emissions of fine particles, NO_x, and CO from on-road vehicles in Finland. *Atmos. Environ.* 39 (35), 6696–6706.
- Zielinska, B., Campbell, D., Lawson, D.R., Ireson, R.G., Weaver, C.S., Hesterberg, T.W., Larson, T., Davey, M., Liu, L.J.S., 2008. Detailed characterization and profiles of crankcase and diesel particular matter exhaust emissions using speciated organics. *Environ. Sci. Technol.* 42 (15), 5661–5666.